

Fabrication, measurement and modeling of electroosmotic flow in micromachined polymer microchannels

Nihal U Suriyage, Muralidhar K Ghantasala, Pio Iovenitti, Erol C Harvey
Industrial Research Institute Swinburne (IRIS), Swinburne University of Technology, P.O. Box 218,
Hawthorn, VIC 3122, Australia
CRC for MicroTechnology, P.O. Box 218, Hawthorn, VIC 3122, Australia

ABSTRACT

Electroosmotic pumping in the microchannels fabricated in polycarbonate (PC), polyethyleneterephthalate (PET) and SU-8 polymer substrates was investigated and species transportation was modeled, in an attempt to show the suitability of low cost polymer materials for the development of disposable microfluidic devices. Microchannels and the fluid reservoirs were fabricated using excimer laser ablation and hot embossing techniques. Typical dimensions of the microchannels were 60 μ m (width) x 50 μ m (depth) x 45mm (length). Species transportation in the microchannels under electroosmosis was modeled by finite element method (FEM) with the help of NetFlow module of the CoventorWareTM computational fluid dynamics (CFD) package. In particular, electroosmosis and electrophoresis in a crossed microfluidic channel was modeled to calculate the percentage species mass transportation when the concentration shape of the Gaussian input species plug and the location of the injection point are varied. Change in the concentration shape of the initial species plug while it is electroosmotically transported along the crossed fluidic channel was visualized. Results indicated that Excimer laser ablated PC and PET devices have electroosmotic mobility in the range 2 to 5 x10⁻⁴ cm²/V.s, zeta potential 30 to 70 mV and flow rates of the order of 1 to 3 nL/s under an electric field of 200 V/cm. With the electroosmotic mobility value of PC the simulation results show that a crossed fluidic channel is electroosmotically pumping about 91% of the species mass injected along one of its straight channels.

Keywords: Electroosmosis, polymer materials, laser ablation, hot embossing, species transportation

1. INTRODUCTION

Electrokinetic flow concepts will have an important role in the future Micro Total Analysis Systems (μ -TAS). A clear understanding and successful realization of micro electroosmotic and electrophoretic flow systems will be the key for the development of many proposed micro bio analysis systems and biochips. Polymeric based disposable devices will be the low cost alternatives for conventional silicon and glass based systems. This has been the motivation for this study on modeling, fabrication and testing of electroosmotic flow in some of the commonly used polymers namely, Polycarbonate (PC), polyethyleneterephthalate (PET) and the negative photoresist SU-8.

1.1 On-chip microfluidic devices

The application of MEMS (Micro Electro Mechanical Systems) technology in the area of life sciences is currently undergoing a revolution, which is expected to become comparable to the vast developments achieved in the field of microelectronics over the last few decades. Microfluidic devices¹⁻⁵, which are analogous to the microchips made of semiconductor material in the latter field, are planar devices with micrometer-sized channels through which fluids are manipulated and analysed. The other main components in a microfluidic system are reservoirs to hold the samples and waste, microchannel network to transport fluids and the fluid control features such as micro-pumps, micro valves and electrodes.

The technological achievements in microfabrication and MEMS technology have seen an application of electrokinetics (explained in 1.2 below) as a method of pumping fluids in microfluidic chips. Electroosmotic pumping in a lab-on-a-chip type device can easily be incorporated into electrophoretic and chromatographic separations. These systems have several distinct advantages over the conventional bench top devices⁶. Most importantly,

- Smaller quantities of samples and reagents are consumed
- Sample losses due to routine sample handling are reduced

- Usage of the chip substrate as a heat sink
- Interference between samples and contamination by the experimenter is minimized (disposable)
- Microfabricated devices enable high throughput sample analysis systems (computer controlled automated systems)

1.2 Electrokinetics - theory

When an electrolyte is in contact with a solid surface, a spontaneous electro chemical reaction occurs between the liquid and the solid surface resulting in redistribution of charges in both the phases ⁶. For conventional microfluidic systems built with glass or fused silica, for example, silanol groups on the surface deprotonate and become electrically negative. An electrical double layer (EDL) is formed by the surface charges of the solid and the liquid immediately adjacent to the solid surface comprising of counter ions as shown in figure 1 below.

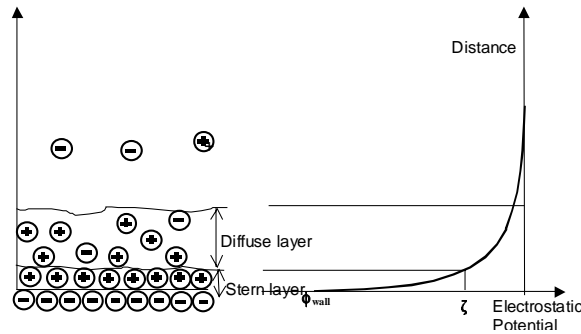


Figure 1: Schematic of an electrical double layer (EDL)

There are two distinctive layers in the liquid phase called Stern and Gouy-Chapman diffuse layers. The thin layer of counter ions in the stern layer are adsorbed to the solid surface with strong electrostatic attraction making them immobile, while counter ions in the diffuse layer are free to move under the influence of an external electric field. The interface between these two layers is called the shear plane and the electrostatic potential at this plane is called the Zeta potential, denoted by the symbol ζ .

Electroosmosis

Electroosmosis is the macroscopic phenomena where the bulk liquid in a capillary is moved with respect to its solid walls with the application of an external electric field along the axis of the capillary. The applied field acts upon the mobile charges in the liquid; as they move in response to the field they drag the bulk liquid with them. The resulting electroosmotic flow velocity, v_{eo} , (in a channel with a finite width EDL and arbitrary cross section that remains constant along the flow direction), is governed by the following equation ⁶.

$$v_{eo} = -\frac{\zeta \epsilon}{\mu} E \quad (1)$$

Where,

ζ	zeta potential of the EDL (V)	ϵ	permittivity of the liquid (F/m)
μ	viscosity of the liquid (kg/m/s) and	E	applied electric field along the capillary (V/m)

1.3 Polymeric substrates for microfluidic devices

In the early part of microfabrication, most of the microfluidic devices were successfully implemented with glass substrates. Glass became the obvious choice as a substrate for these microstructures due to its optical transparency, stability at high temperatures, chemical resistivity and high electrical resistivity. In addition to these, glass as a material has the biggest advantage of compatibility with the existing fabrication technologies employed in the semiconductor industry. Standard photolithography and subsequent wet chemical etching processes are proven technologies with Si

substrates, are readily available and applicable with glass or quartz substrates. These steps can also be automated and batch-processed with the existing fabrication facilities for mass production. When it comes to lab-on-a-chip type applications, however, glass or quartz materials have several major disadvantages⁷. Firstly, cost of materials is too high to be used as disposable devices. The next problem is the large number of steps involved in the fabrication process such as cleaning, resist coating, photolithography, development and wet etching. Higher number of steps will increase the fabrication time and hence lower throughput in the mass production. Further, these serial steps will increase the probability of fabrication errors in the final product. The existing fabrication technologies on glass substrates have limitations in geometrical design due to the isotropicity of the etching process. For microfluidic applications, channels with square cross section, high aspect ratio or channels with different heights may be desirable. But existing wet chemical etching on glass or quartz materials cannot yield these results. In addition to the geometry, surface chemistry of etched glass channels also creates a problem for biopolymer separations by adsorbing biomolecules to the negatively charged channel walls.

These disadvantages have led the research world to explore new materials and fabrication methods to overcome the above problems and commercialize microfluidic devices. Over the last few years polymers have become the most promising material for this purpose. Most of the microstructures have been implemented on commonly available polymer materials such as polyethylene (PE), polycarbonate (PC), polyethyleneterephthalate (PET), polystyrene (PS), cellulose acetate, polyamide (PA), polymethylmethacrylate (PMMA) and poly dimethylsiloxane (PDMS). This paper investigates the ability of electroosmotic pumping of fluids in microchannels fabricated in PC, PET and the negative photoresist SU-8.

1.4 Simulation of electroosmosis

Rapid advancements in microfluidic devices have given rise to the need of simulating the electrokinetic effects in these devices. Injecting a chemical or biological sample (species) to the separation channel of an electrophoresis chip or transportation of a DNA strand to a processing node of a DNA extraction chip are two basic examples of such applications. Simulating these systems can facilitate the system designers and scientists by saving their valuable time and cost in building prototypes, visualizing and understanding how fluids behave in microfluidic networks as well as optimizing the system parameters of the final product.

The NetFlow module in CoventorWareTM is specifically used for the simulation and design of interconnects for chemical transport of species in microchannels. The physical phenomena associated with the transport in microfluidic devices include⁸

- Pressure flow
- Diffusion
- Electrophoresis
- Electroosmosis and
- Dielectrophoresis.

In NetFlow these phenomena can be modelled individually or in combination. Solutions to microfluidic problems are solved using the Navier-Stokes equation for flow, the mass equation for species motion and the Poisson equation for electric field. Electroosmosis and electrophoresis are modelled by their respective coefficients.

This paper investigates the effects to a species plug transported along one of the arms of a crossed microfluidic channel. The perpendicular intersection of two microchannels is of special interest for two reasons: first it represents the fundamental unit of a more complicated grid like microchannel networks; and second, it may be used in conjunction with electroosmotic flow to facilitate discrete sample injections into microfluidic devices.

1.5 Measurement of electroosmosis

It can be shown that electrical current in the microchannel under an electric field applied tangentially to the solid liquid interface is directly proportional to the current due to the mobile ions in the EDL⁹. This concept was first employed by Huang et al.¹⁰ to measure the electroosmotic mobility in a capillary. This method of measuring electroosmosis is called the "current monitoring method" and is summarized below.

Figure 2 shows the schematic diagram of an experimental set up used in this experiment. First, input reservoir, microchannel and the output reservoir are filled with a buffer solution of concentration C_1 (Mol/l) and turn on the external electric circuit. A constant current will result depending on the applied voltage. If input reservoir is emptied and

filled with another solution with slightly higher concentration of C2 (Mol/l), current in the channel will increase until the whole channel is filled with the new solution (current will decrease in the same way if C2 is less than C1). The time taken for this change in current is the time (T) taken by new buffer solution to travel from input to the output, or length of the channel, L. Electroosmotic velocity and electroosmotic mobility can be calculated by equations 2 and 3 respectively.

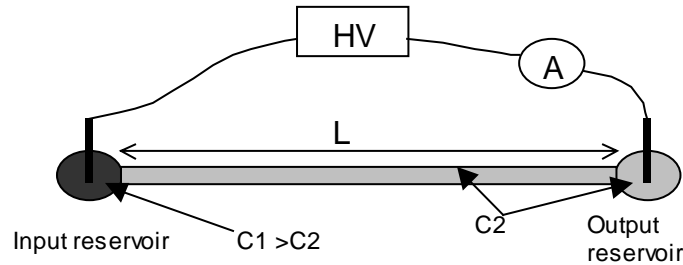


Figure 2: Experimental set up for current monitoring method. HV - high voltage power supply, A - ammeter

$$v_{eo} = L/T \quad (2)$$

and electroosmotic mobility

$$\mu_{eo} = v_{eo} / E. \quad (3)$$

Where, E is the applied electric field (V/cm).

2. EXPERIMENTAL

2.1 Fabrication of microfluidic devices

Figure 3 below shows the schematic diagram of the microfluidic device fabricated for this experiment, which has three reservoirs (input, output and side arm) and two microchannels connecting them. A 45mm long channel from input to the output reservoirs was used to measure the electroosmosis, while side arm channel and the reservoir was designed to get rid of the air bubbles in the main channel and refresh the buffer solutions during experiments. These channels and reservoirs were fabricated in polymer substrates by excimer laser ablation and hot embossing techniques as described below. Electrodes for input and output reservoirs were cut from an adhesive 25 mm copper tape (3M, 35 μ m thick single sided adhesive) and stuck on the cover plate of the device to be inserted into the reservoirs filled with carrier buffer only during electroosmotic pumping. This arrangement was used to minimize oxidation of copper and consequent channel blockage due to debris pushed into the channel when buffer solution is forced into the device using a disposable syringe.

Excimer laser ablation

Polycarbonate and PET devices fabrication: Polycarbonate (1.6mm thick sheets from GE Polymer Shapes), PET (250 μ m thick sheets from Toray Industries) and SU-8 (SU-8 2150 form Micro-Chemical Corporation) devices were micromachined by laser ablation using a Series 8000 (Exitech Ltd, UK) excimer laser workstation. The laser (Lambda Physik, LPX 210i, Germany) operated at a wavelength of 248nm, with a 20 ns pulse (FWHM) and pulse energy densities of up to 2.0J/cm². Chrome on quartz and metal masks with rectangular shapes were used and the patterns were demagnified by a factor of x10. CNC control of the system allowed for a combination of static and mask-dragging ablation processes in order to construct reservoirs and channels respectively. Laser fluence and number of shots per area were controlled to achieve 40 μ m depth in the reservoirs and 50 μ m depth in the channels. Polycarbonate and PET devices were sealed by diffusion bonding with a cover plate of the same material. Openings for fluid reservoirs were mechanically drilled though these plates before thermally bonding them to the base plate in an in-house hot embossing machine. Temperature and pressure for this process were 130 °C and 60-65 bars for polycarbonate while 190 °C and 60-65 bars for PET.

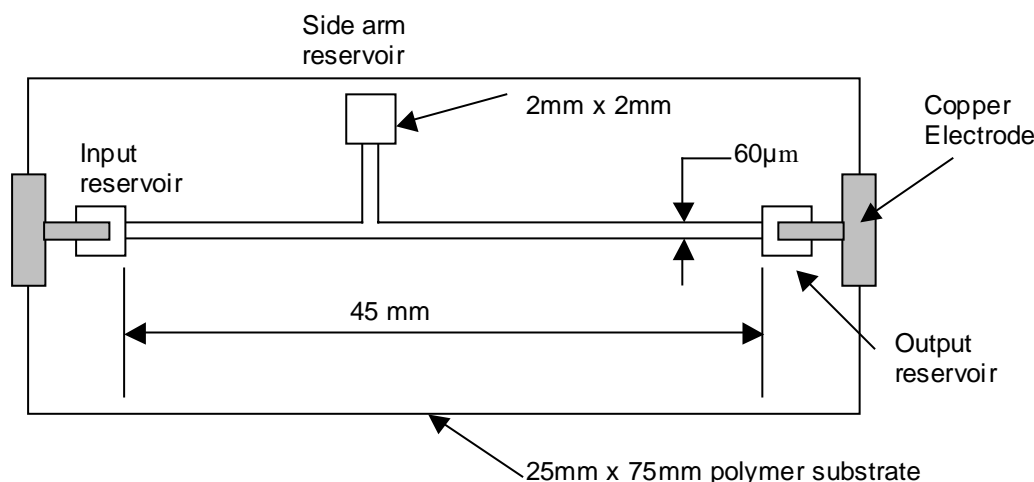


Figure 3: Schematic diagram of the microfluidic device fabricated for the measurement of electroosmotic mobility in polymer substrates (not to scale)

SU-8 device fabrication: An adhesive layer of XP omnicoat (Micro-Chemical Corporation) was spin coated (spin coater P6700 from Speciality Coating Systems) on a cleaned polycarbonate sheet and was pre-baked in a vacuumed oven for 2 minutes at 200 °C. A 100µm thick SU-8 layer was spin coated on the XP omnicoat layer and pre-baked at 65 °C for 5 minutes and then soft-baked at 95 °C for another 30 minutes for solvent evaporation from the thin film. This sample was then excimer laser machined to fabricate the reservoirs and channels. A cover plate was prepared by spin coating a 5µm layer of SU-8 on a second polycarbonate sheet. With mechanically drilled holes for fluid connections on the cover plate, substrate and the cover plate were blanket exposed to UV light in a UV exposure chamber to polymerize SU-8 layers. Sealing of the device was achieved by the post exposure bake (PEB) of SU-8 layers, which were kept facing each other (see figure 4) at 65 °C for 1 minute and then at 95 °C for 15 minutes in the oven, while applying a slight pressure using four alligator clips.

Hot embossing

Polycarbonate and PET substrates were used to hot emboss the same microfluidic device using an electroplated Nickel shim. Top and bottom plates of the embossing tool (see figure 5) were preheated to the required temperature and the pressure control device was programmed with the upper and lower pressure limits. Substrate and the nickel shim were kept in the middle cavity facing each other as shown in the diagram. Table 1 shows the temperature, pressure and duration values used with each substrate to obtain well defined channels and reservoirs.

Substrate	Pressure (Bars)	Temperature (°C)	Duration (Minutes)
Polycarbonate	60 - 65	160	30
PET	70 - 75	195	30

Table 1: Hot embossing parameters for polycarbonate and PET substrates

2.2 Measuring electroosmosis

Current monitoring method explained in the section 1.5 was employed to measure electroosmotic mobility in all the devices fabricated. Phosphate buffer solution with 0.05M and 0.04M was used as C1 and C2 respectively. A disposable syringe and a locally made fluid connector were used to fill channels and the reservoirs. High voltage power supply (0-

10kV) and a multimeter (fused 0-200 μ A range) were connected in series with the microchannels (filled with a fluid) to make a closed electrical circuit. After each measurement the whole system was refreshed with original buffer solution for three times to restore the electrical double layer (EDL) to its original condition. Time measurements were carried out 5 times by filling channels and reservoirs with the higher concentrated buffer (C1) and then replacing the input reservoir with lower concentrated buffer (C2). Another 5 readings were taken with the same device by interchanging the buffer solutions C1 and C2. Finally, the average of these 10 readings was taken as the time T to fill the channel with new buffer solution.

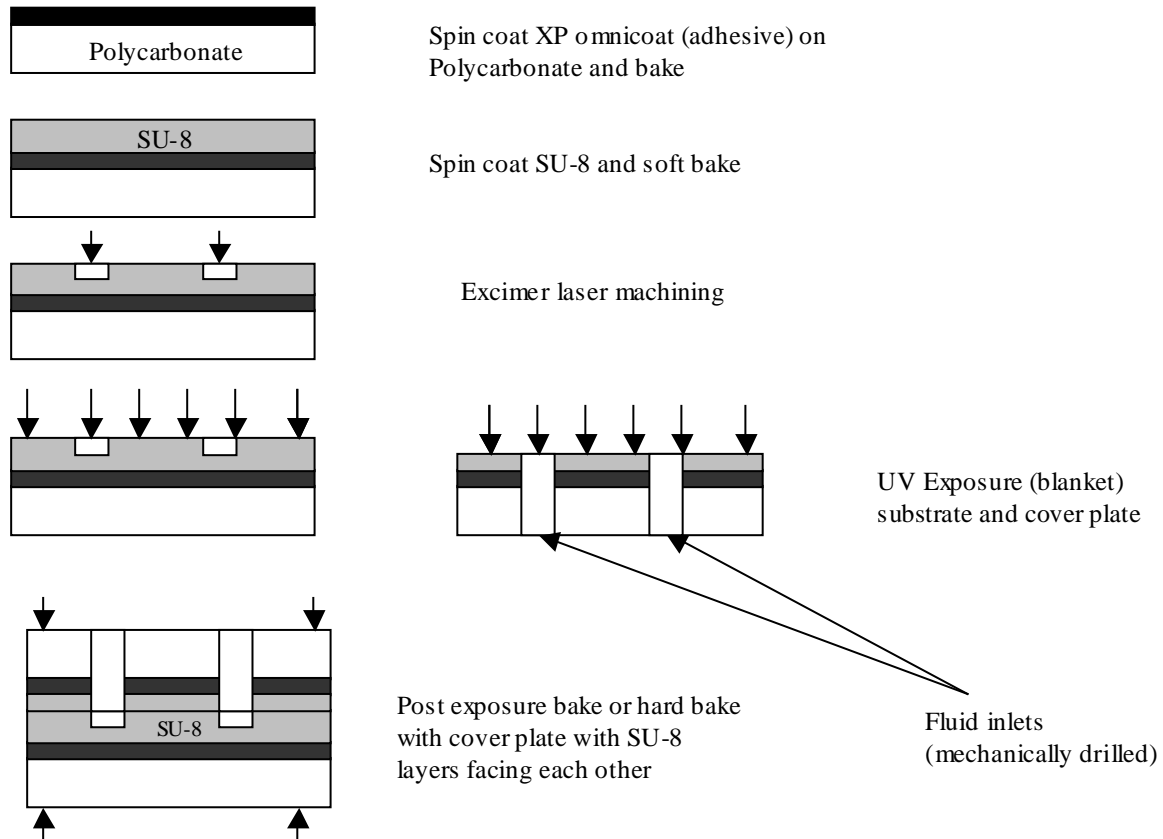


Figure 4: Fabrication steps of microfluidic devices in SU-8 thin films on Polycarbonate substrate

2.3 Simulation of species transport in the crossed microfluidic channel

Figure 6 below shows the details of the crossed microchannel system used for simulation in this experiment, which has 50 μ m wide channels with each arm 250 μ m in length. Four reservoirs were connected to the ends of the channels, and channel from A to B is used to transport a species plug, which was placed at distance x μ m from the center of the channel intersection. Electroosmosis was modeled by using the electroosmotic mobility of the buffer solution, which is given as a Wall Effect in the NetFlow software. An electric field was simulated along the channel AB by assigning a voltage difference of 20V as boundary conditions at the input and output. This is equal to an electric field of $20/0.05 = 400$ V/cm for electroosmosis and electrophoresis, which carries the species along the channel. The direction of electroosmosis depends on the net surface charges on the wall and the electrophoresis direction is decided by the polarity of the species. Table 2 has the details of all the constant parameters and the NetFlow sign conventions used for this simulation model.

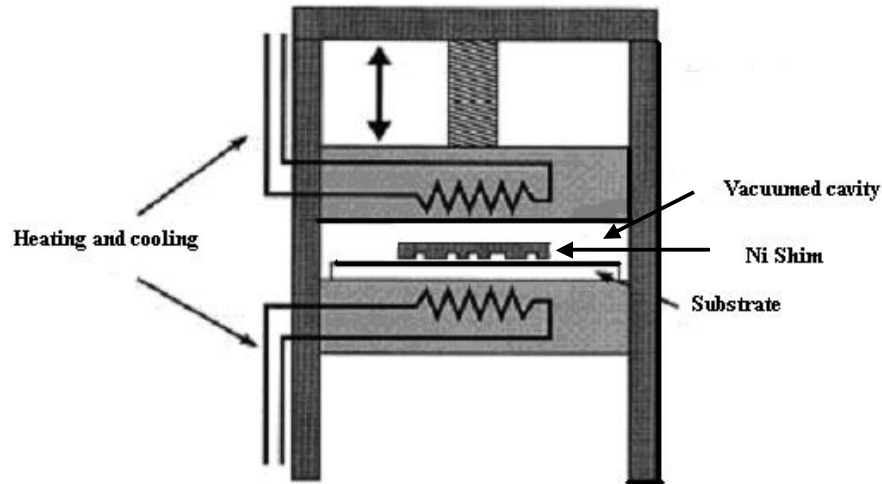


Figure 5: Schematic Diagram of the in-house hot Embossing System used to fabricate microfluidic devices for electroosmotic mobility measurements

Four different variables were chosen for this simulation. Three of them were the dimensions of the Gaussian species plug: amplitude, standard deviation, and flat peak. The injection point of the plug (marked “x” in figure 6) was considered to be the fourth variable. With the varying values of each four parameters above, the crossed channel was simulated in NetFlow transient analysis and the percentage species mass transported to the output after three seconds was calculated using finite element method (FEM). The species plug shape (concentration as a mass fraction) along the channel and at the crossed intersection was also visualized.

Parameter	Value	Comments
Electroosmotic Mobility (μ_{eo})	$+4.5 \times 10^{-4} \text{ cm}^2/\text{V.s}$	Value found in 3.1 (our results) for excimer laser ablated polycarbonate samples + Sign means NetFlow assigns the direction of Electroosmosis from A \rightarrow B (Negative channel walls)
Electrophoretic Mobility	$+1.5 \times 10^{-4} \text{ cm}^2/\text{V.s}$	+ Sign in NetFlow means negative species and move from B \rightarrow A
Diffusion Coefficient	$5 \text{ } \mu\text{m}^2/\text{s}$	
Molecular Weight of Species	500 a.m.u	
Electric field	400 V/cm	20 V from A \rightarrow B; Electric field = (20V/500 μm)

Table 2: Constant electrokinetic parameters employed in the NetFlow simulation of species transportation; sign for each quantity is assigned in accordance with the NetFlow sign conventions.

3. RESULTS

3.1 Electroosmotic mobility measurements

Figure 7(a) below depicts the typical set of curves plotted with our results of current monitoring method for microchannels in polycarbonate sample. These curves resulted from the five measurements taken by first filling the channels and reservoirs with less concentrated buffer (0.04M) and then replacing the input reservoir by a slightly higher (0.05M) concentrated buffer. The expected constant current at the beginning of the curve is missing due to the fact that measurements were started (time = 0) just after the input reservoir was filled with the second buffer solution. The

average time taken by the current to reach the steady state was used to calculate the electroosmotic mobility by using equation (3). The Zeta potential for the liquid-solid interface, ζ was calculated by equation (1) with the relative permittivity value of 76.5 (measured using HP 8410 Network Analyzer) and assuming a viscosity of $10^{-3} \text{ Nm}^{-2}\text{S}$ (water). Figure 7(b) shows an optical microscope image of an excimer laser machined microchannel connected to a reservoir in PET substrate.

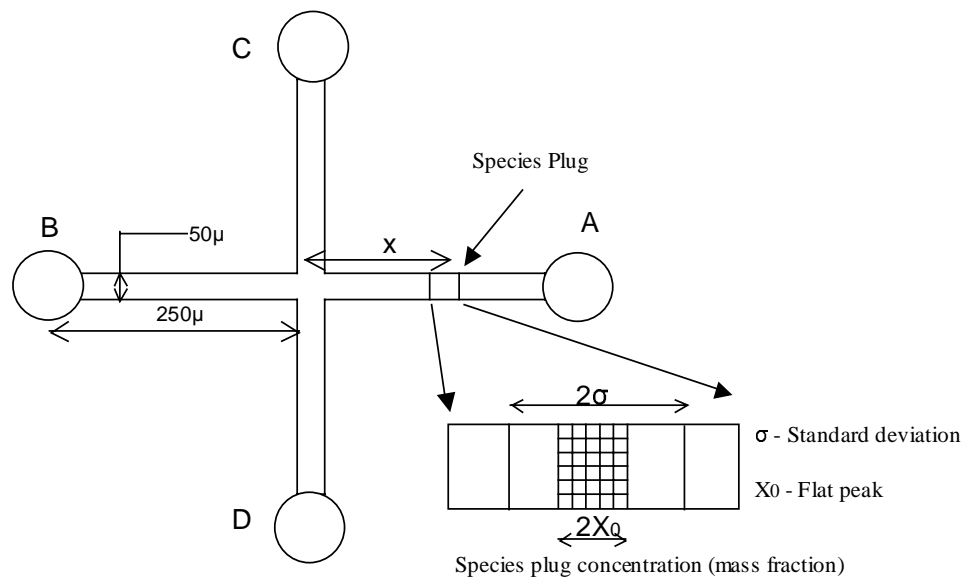


Figure 6: Schematic diagram showing the model used to simulate species transportation in the crossed fluidic channel

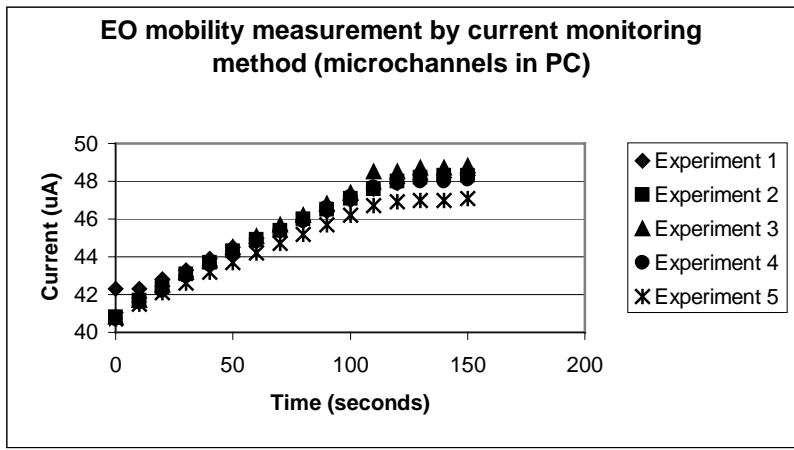


Figure 7: (a) Results of current monitoring method experiments for excimer laser ablated microchannels in polycarbonate substrate

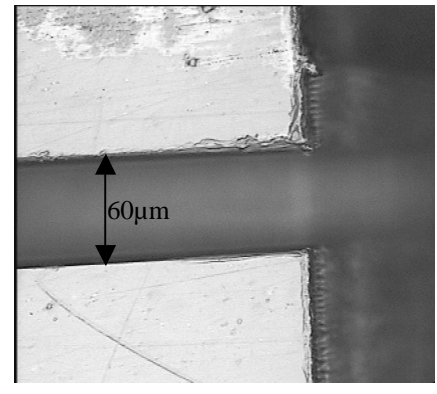


Figure 7 (b): An optical microscope image of excimer laser ablated channel connected to the output reservoir in PET substrate

Table 3 below summarizes the results obtained for samples fabricated with different substrate and fabrication method combinations. Excimer laser ablated polycarbonate channels have the highest electroosmotic mobility of $(4.5 \pm 5\%) \times 10^{-4} \text{ cm}^2/\text{V}\cdot\text{s}$ among these three materials. Microchannels in both PC and PET fabricated using a hot embossing technique have a less electroosmotic mobility than their respective values for laser ablated channels. This can be attributed to the fact that the excimer laser ablation (mask dragging) process produces a hydrophilic surface chemistry in the microchannel¹¹, which has improved the electroosmosis in the channel. Hot embossed channels, on the other hand, have slightly less electroosmotic mobility due to less wettability in the channel surface, but the hot embossing process is considered to be one of the widely used cost effective mass production techniques applicable to a wide range of polymer materials. Depending on the material and fabrication method, microchannels used in our experiments show that PC and

PET substrates can support an electroosmotic flow rate in the range 1.4 – 3.0 nL/s at 200 V/cm electric field. It was a time consuming exercise to seal the SU-8 device without blocking the microchannels. In most of our samples, channels were blocked due to the flow of the material. More work should be done to optimize this procedure of making microfluidic devices with SU-8 as the structural layer.

Material/Fabrication Method	Electroosmotic Mobility ($10^{-4} \text{ cm}^2/\text{V.s}$)	Flow Rate (nL/s) @ 200 V/cm electric field	Zeta Potential (mV)
Polycarbonate/ Excimer laser	$4.5 \pm 5\%$	2.97	66.47
Polycarbonate/ Hot embossing	$3.1 \pm 8\%$	2.05	45.79
PET/ Excimer laser	$2.5 \pm 8\%$	1.65	36.93
PET/Hot embossing	$2.1 \pm 8\%$	1.39	31.02
SU-8/Excimer laser	$1.1 \pm 7\%$	0.70	15.66

Table 3: Electroosmotic mobility of polymeric microfluidic channels measured using current monitoring method

3.2 Simulation

Figure 8 shows the percentage mass transportation results for four different cases simulated in this experiment. Figures 8(a) – (c) explain how the percentage mass transportation varies when the shape of the input species plug is changed. It has been observed that there is a very small effect on the output when amplitude (A), flat peak (x0) or the standard deviation (σ) of the plug is changed. Nearly 91% of the input mass is transported to the output.

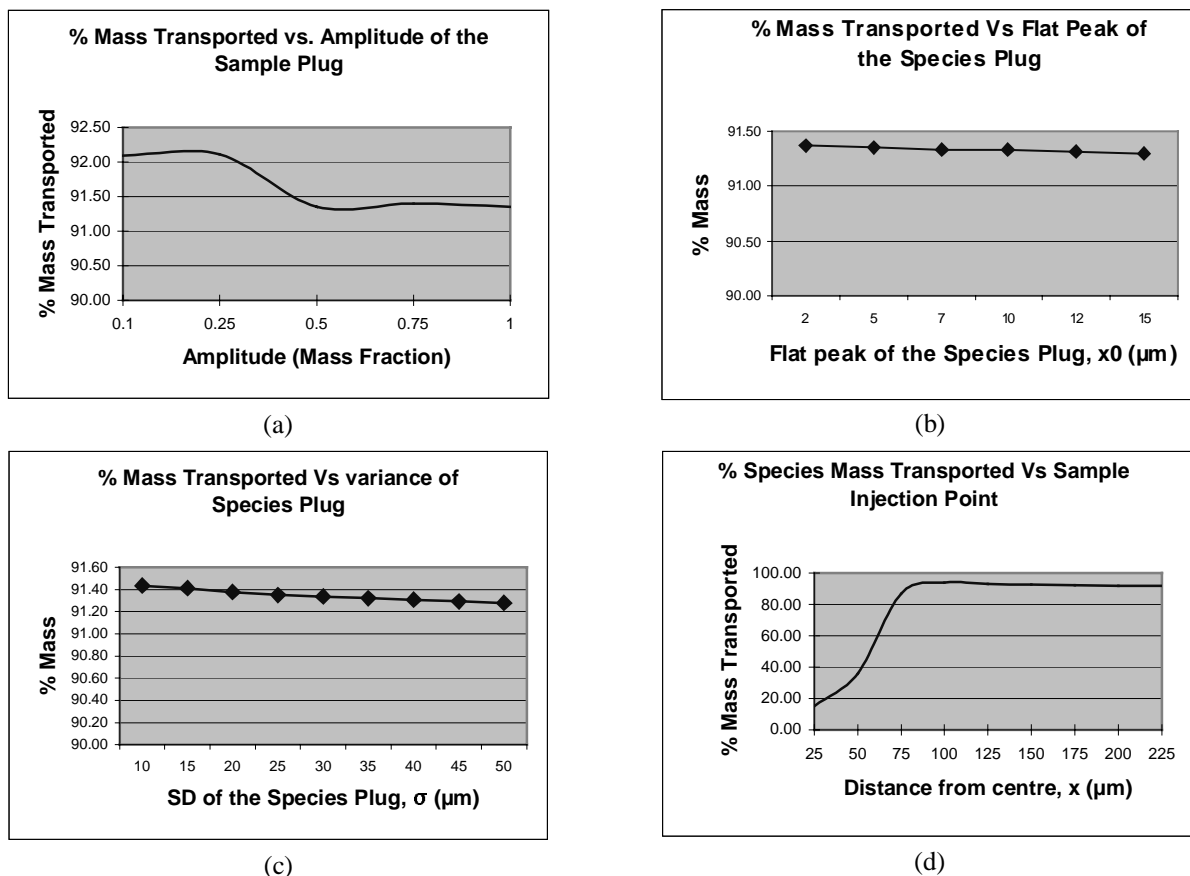


Figure 8: Results of the simulation performed on a Gaussian species plug injected into a crossed microfluidic channel showing percentage mass transported by electroosmosis under four different scenarios. (a) Amplitude of the species plug (b) Flat peak of the species plug (c) Standard deviation of the species plug (d) Injection point of the microchannel

Figure 8(d) indicates that injection point does affect the results. It is seen that the injection point should at least about 90 μm away from the center of the channel intersection to obtain the maximum mass transportation ($\sim 91\%$). This is mainly due to the diffusion of the species into the crossed channel (CD in figure 6 above) in the injection process before gaining the electroosmotic velocity. This situation is visualized in figure 9, which shows the first, $t=0$, 9 (a) and the last, $t=3$ sec 9 (b) frames of the simulation for the case of $x = 50 \mu\text{m}$. It is clearly seen from figure 9 (b) that a considerable amount of species is resident in the crossed section of the channel (CD) after 3 seconds. If we compare the equivalent frames from the simulation for the case of $x = 150 \mu\text{m}$ (figure 10 (a) and (b)) where nearly 91% of the mass is carried to the output after 3 seconds, a very small amount of species mass is resident in the perpendicular channel.

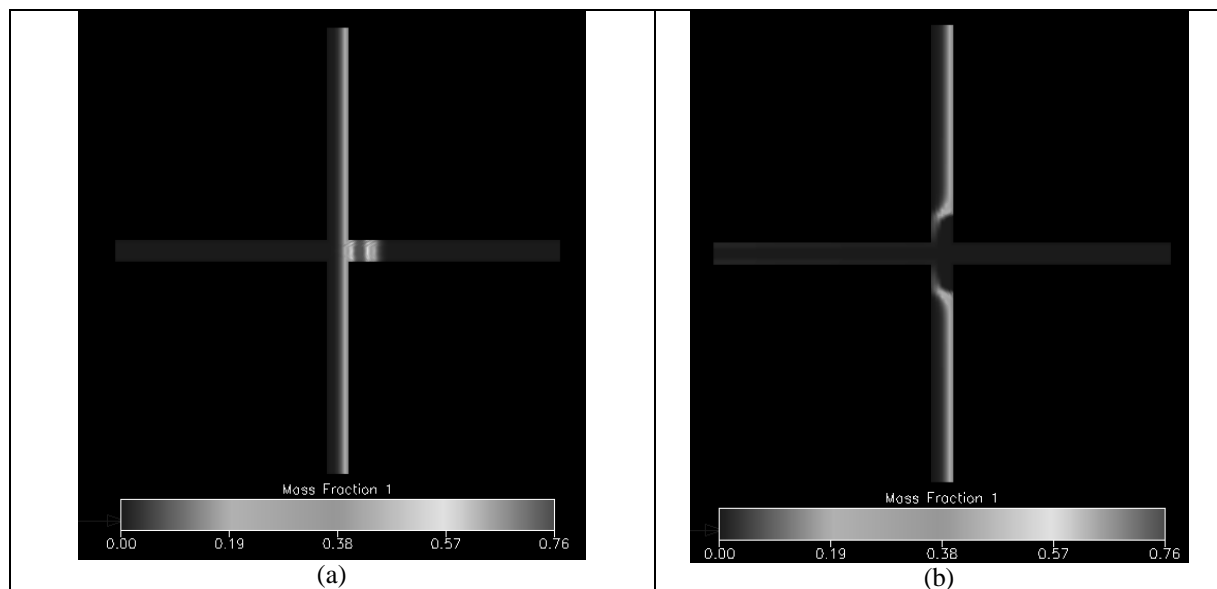


Figure 9: First (a), $t = 0$, and the last (b), $t = 3\text{sec}$, frames showing species mass distribution in the crossed microfluidic channel for the case of $x = 50 \mu\text{m}$. A large proportion of the initial species mass is introduced to the crossed channel CD as seen in (a). After 3 seconds, the crossed channel still carries a considerable amount of species in (b).

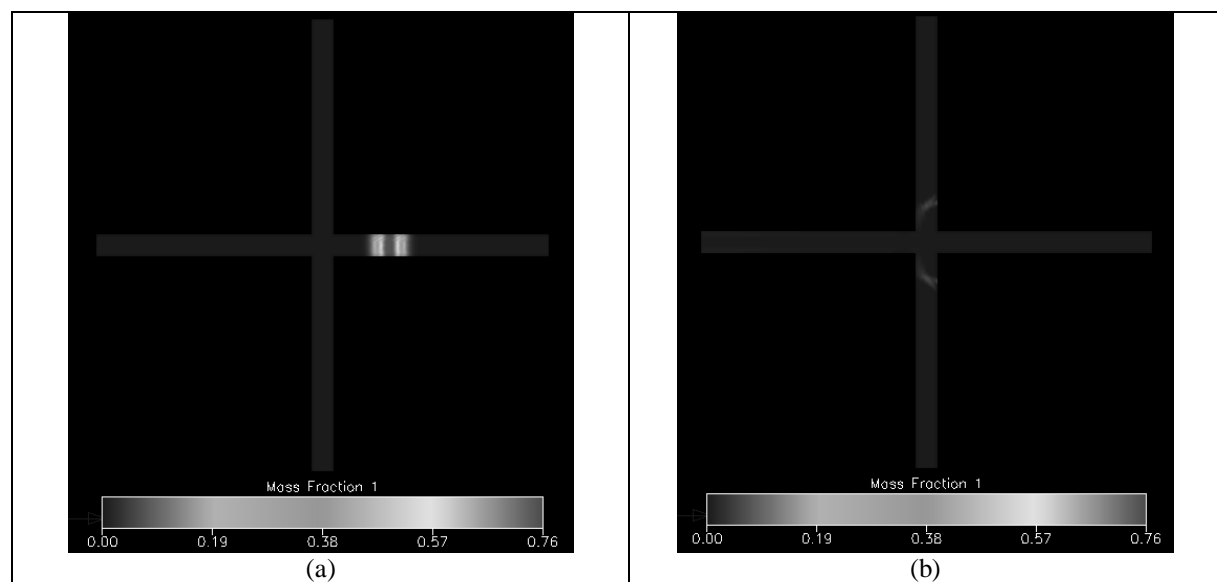


Figure 10: First (a) $t = 0$, and the last (b) $t = 3\text{sec}$, frames showing species mass distribution in the crossed microfluidic channel for the case of $x = 150 \mu\text{m}$. Only a small percentage ($\sim 9\%$) of the initial mass is resident after 3 seconds in the crossed channel.

The shape of the species plug is greatly changed at the intersection of the channels due to diffusion into the crossed channel. The flat peak section is reduced in area and concentration after the intersection and a pointed head is formed from the body of the species plug and; in this new shape there is a considerable increase in the length of the plug as it approaches the output reservoir as shown in figures 11(a) \rightarrow (d).

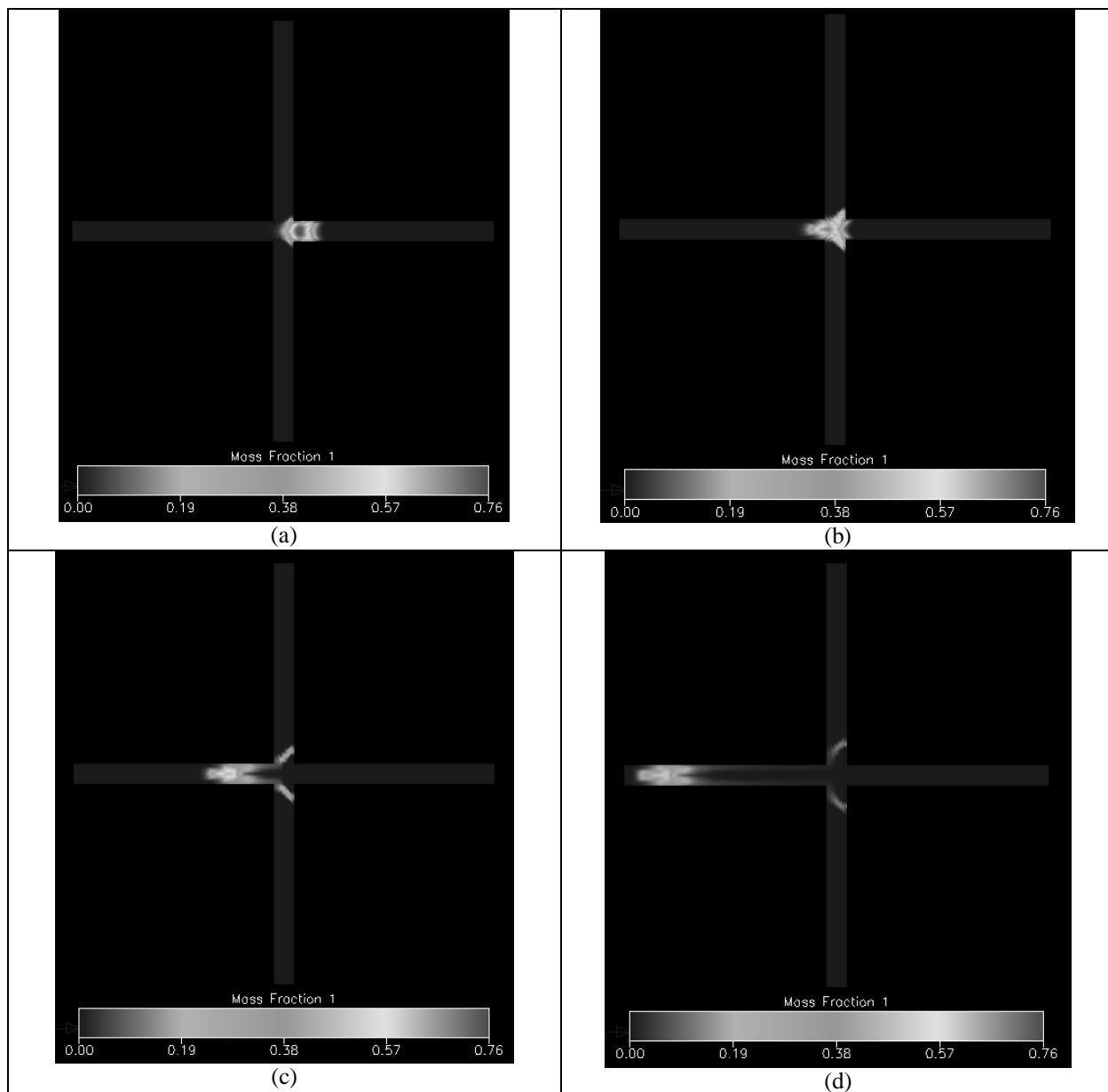


Figure 11: Frames from the simulation showing the changes to the shape (concentration as a mass fraction) of the species plug at the crossed intersection of the microchannels. Shape of the plug just entered the intersection (a), the flat peak of the plug is distributed at the intersection (b), small head is formed and part of the plug is diffused into the crossed channel (c), and final length of the plug is increased due to diffusion along the channel (d)

CONCLUSIONS

Microfluidic channels and reservoirs were successfully fabricated in polymeric substrates using excimer laser ablation and hot embossing techniques, and electroosmotic mobility of a standard carrier buffer was measured using a current monitoring method. Finite element method was used to visualize and calculate percentage mass transportation of an electroosmotically-transported species along an arm of a crossed microfluidic channel. Electroosmotic pumping found to be a good method of transporting species in low cost microfluidic devices fabricated in PET and PC substrates. A Thin film of SU-8 spin coated on polycarbonate substrate can be excimer laser machined to act as the structural layer of microfluidic devices when the parameters of the sealing process are optimized.

ACKNOWLEDGEMENTS

Authors would like to acknowledge all the support extended by the CRC for Microtechnology, and colleagues at Industrial Research Institute Swinburne (IRIS), especially, Sebastiaan Garst, Martin Telgarsky and Abdirahman Yussuf for their kind help in support of our experiments.

REFERENCES

1. Chan, J. H., Qin, T. D., and Aegersold, R., " Microfabricated Polymer Devices for Automated Sample Delivery of Peptides for Analysis by Electrospray Ionization Tandem Mass Spectrometry ", *Analytical Chemistry*, **71**(20), 4437-4444, 1999.
2. Kamei, T., Paegel, B. M., Scherer, J. R., Skelley, A. M., Street, R. A., and Mathies, R. A., " Integrated Hydrogenated Amorphous Si Photodiode Detector for Microfluidic Bioanalytical Devices ", *Analytical Chemistry*, **75**(20), 5300-5305, 2003.
3. Manz, A., Effenhauser, C. S., Burggarf, N., H., Jed D., Seiler, K., and Fluri, K., " Electroosmotic Pumping and Electroosmotic Separations for Miniaturised Chemical Analysis Systems ", *J. Micromech, Microeng*, **4**, 257-265, 1994.
4. McClain, M., M., Christopher T., J., Stephen C., and Ramsey, M. J., " Flow Cytometry of Escherichia coli on Microfluidic Devices ", *Analytical Chemistry*, **73**(21), 5334-5338, 2001.
5. Rossier, J. S., Schwarz, A., R., Frederic, F., R., Bianchi, F., and Girault, H. H, " Microchannel Networks for Electrophoretic Separations ", *Analytical Chemistry*, **20**, 727-731, 1999.
6. Sharp, K. V., Ronald J. A., Santiago, J. G., and Molho, J. I., " *The MEMS Handbook*, Editor Mohamed Gad-el-Hak, 6-19-24. London: CRC Press, 2002.
7. Becker, H., and Gartner, C., "Polymer Microfabrication Methods for Microfluidic Analytical Applications." *Analytical Chemistry*, **21**(1), 12-26, 1999.
8. CoventorWare, *Microfluidic Reference Guide*, F3-37- 40. California: CoventorWare Inc., 2001.
9. Ramsey, R. S., and Ramsey, J. M., " Generating Electrospray From Microchip Devices Using Electroosmotic Pumping." *Analytical Chemistry*, **69**(6), 1174-78, 1997.
10. Huang, X., Gordon, M.I J., and Zare, R. N., " Current Monitoring Method for Measuring the Electroosmotic Flow Rate in Capillary Zone Electrophoresis." *Analytical Chemistry*, **60**(17), 1837-1838, 1988.
11. Wagner, F, and Hoffmann, P., " Structure Formation in Excimer Laser Ablation of Stretched Poly (Ethylene Terephthalate): the Influence of Scanning Ablation. " *Applied Physics A*, **A69**, S841-S844, 1999.